Searching Appropriate Mother Wavelets for Hyperanalytic Denoising

Ioana FIROIU[1,2], Corina NAFORNITA[1], Jean-Marc BOUCHER[2], Alexandru ISAR[1]
[1]*Politehnica University of Timisoara, 300223, Romania*
[2]*Telecom Bretagne, Brest, France*
alexandru.isar@etc.upt.ro

***Abstract*— The aim of this paper is the association of a new variant of Hyperanalytic Wavelet Transform (HWT) with a maximum a posteriori (MAP) filter, named bishrink for the denoising of images affected by additive white Gaussian noise (AWGN). The best results are obtained with the biorthogonal mother wavelets Daubechies 9/7.**

***Index Terms*— Wavelet transforms, Hilbert transforms, White noise, Filtering, MAP estimation.**

I. INTRODUCTION

During acquisition and transmission, images are often corrupted by additive noise. The aim of an image denoising algorithm is then to reduce the noise level, while preserving the image features. The acquired image is expressed as:

$$f = s + n,$$

where s represents the noiseless input image and n the noise. Generally n is considered as AWGN. Computing a WT of both members of the last equation, its equivalent form is obtained:

$$y = w + n,$$

where y=WT$\{f\}$ and n=WT$\{n\}$, because the WT is linear and the WT of AWGN is also AWGN, [1].

One may classify the denoising systems in two categories: those directly applied to the signal [2] and those who use a wavelet transform before processing. The multi-resolution analysis performed by the WT is a powerful tool to achieve good denoising. In the wavelet domain, the noise is uniformly spread throughout the coefficients, while most of the image information is concentrated in the few largest ones (sparsity of the wavelet representation). Soft-thresholding filter (stf) is the most popular strategy to denoise in the wavelets domain and has been theoretically justified by Donoho and Johnstone [1]. They propose a three steps denoising algorithm:

1) the computation of the forward WT,
2) the filtering of the wavelet coefficients,
3) the computation of the inverse WT (IWT) of the result obtained.

They use the Discrete Wavelet Transform (DWT) and the stf. This method can be considered non-parametric. Consequently, regarding the three steps denoising algorithm, there are two tools to be chosen: the WT and the filter. In what concerns the first choice, in this paper we will use a new implementation of the HWT [3]. In [4] was used the 2D Undecimated Wavelet Transform (2D UDWT), in [5] the 2D Double Tree Complex Wavelet Transform (2D DTCWT), and in [6] the 2D DWT. Concerning the second choice, numerous non-linear filter types can be used in the WT domain. Basically, there are two categories of estimators: non-parametric and parametric. From the first category can be mentioned: the hard-thresholding filter, [1], the stf [1], the Efficient SURE-Based Inter-scales Point-wise Thresholding Filter [6], and the filter proposed in [7]. To the second category belong filters obtained by minimizing a Bayesian risk under a cost function, typically a delta cost function (MAP estimation [4, 5]) or the minimum mean squared error (MMSE estimation [6]). We have already associated the proposed implementation of HWT with a marginal MAP filter in [3]. The aim of this paper is to improve the results in [3] by the substitution of the marginal MAP filter with the bishrink filter [5].

The structure of the paper is the following. In the second section we present the new version of the HWT. In the third section we recall the bishrink filter. The fourth section is dedicated to simulation results. Finally, the last section summarizes our conclusions.

II. PROPOSED WT

Any WT of a 1D real signal can be generalized to an analytical WT if the mother wavelets used for the computation of the former WT is replaced by its associated analytical function. Analytical mother wavelets are already constructed and analyzed for the Continous Wavelet Transform [8]. We have proposed a different construction of analytic mother wavelets in [3] and we have proved that an analytical 1D DWT of a real signal can be computed by applying a real 1D DWT to the analytical signal associated to the input signal. In the following we will use the definition of the analytic signal associated to a 2D real signal named hypercomplex signal. This definition is not unique. Hyperanalytic mother wavelets have four components, each one localized in a different quadrant of their 2D spectrum. Dealing with four components, the construction of the hyperanalytic mother wavelets must be based on an algebra whose elements are sets of four numbers. Choosing different algebras, different definitions of the hyperanalytic signal are obtained. In [9] and in other studies the algebra of quaternions was chosen. We have preferred in [3] the 4-D **commutative hypercomplex algebra** proposed in [10]. An element of this algebra and its conjugate can be expressed as:

This work was supported in the framework of a grant funded by the Romanian research council (CNCSIS) with the title "Using wavelets theory for decision making" no. 349/13.01.09.

$$
\begin{aligned}
&Z = 1x + \dot{\imath}y + \dot{\jmath}z + \dot{k}u\ ;\\
&Z^{*} = 1x - \dot{\imath}y - \dot{\jmath}z + \dot{k}u\ ;\\
&Z = \left[(x-u)+i(y+z)\right]\left(\frac{1-\dot{k}}{2}\right)+\\
&+\left[(x+u)+i(y-z)\right]\left(\frac{1+\dot{k}}{2}\right).
\end{aligned}
\tag{1}
$$

The last equation in (1) expresses the element Z in the canonical form. The hypercomplex mother wavelet associated to the real mother wavelet $\psi(x,y)$ is defined as:

$$
\begin{aligned}
&\psi_h(x,y) = 1\cdot\psi(x,y) + i\cdot\mathcal{H}_x\{\psi(x,y)\}+\\
&+j\cdot\mathcal{H}_y\{\psi(x,y)\}+\dot{k}\cdot\mathcal{H}_x\{\mathcal{H}_y\{\psi(x,y)\}\}
\end{aligned}
\tag{2}
$$

where $i^2 = j^2 = -\dot{k}^2 = -1$, $ij = ji = \dot{k}$, $j\dot{k}=\dot{k}j=-i$, $\dot{k}i=i\dot{k}=-j$, and $ij\dot{k}=1$, [10]. The HWT of the image $f(x,y)$ is:

$$
HWT\{f(x,y)\} = \langle f(x,y), \psi_h(x,y)\rangle. \tag{3}
$$

Taking into account (2) and (3), it can be written:

$$
\begin{aligned}
&HWT\{f(x,y)\} = DWT\{f(x,y)\}+\\
&iDWT\left\{\mathcal{H}_x\{f(x,y)\}\right\}+jDWT\left\{\mathcal{H}_y\{f(x,y)\}\right\}+\\
&+kDWT\left\{\mathcal{H}_y\left\{\mathcal{H}_x\{f(x,y)\}\right\}\right\}=\\
&\langle f_h(x,y), \psi(x,y)\rangle = DWT\{f_h(x,y)\}.
\end{aligned}
\tag{4}
$$

The HWT of the image $f(x,y)$ can be computed with the aid of the 2D-DWT of its associated hypercomplex image. So, the proposed HWT variant represents the generalization of our analytical WT transform [3]. The new HWT implementation, [3], presented in Fig. 1, uses four trees, each one implementing a 2D-DWT. The first tree is applied to the input image. The second and the third trees are applied to 1D discrete Hilbert transforms computed across the lines ($\mathcal{H}_x$) or columns ($\mathcal{H}_y$) of the input image. The fourth tree is applied to the result obtained after the computation of the two 1D discrete Hilbert transforms of the input image. These are initial computations. To obtain an enhanced directional selectivity, some additional linear operations, represented in the right part of Fig. 1, must be performed [11]. The result is composed by two sequences of complex

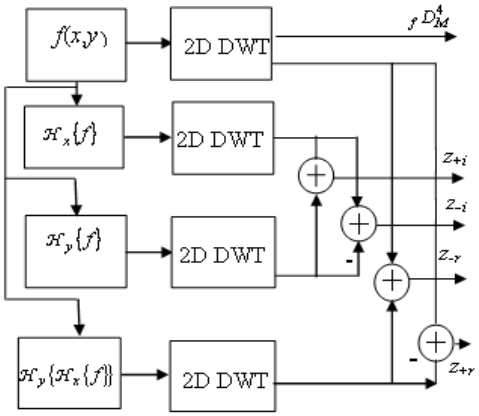

Initial computations Directional selectivity Enhancement

Fig. 1. The new HWT implementation.

coefficients:

$$
\begin{aligned}
&z_{+} = z_{+r} + jz_{+i} =\\
&=\left(f\,D_m^{1,2,3} - \mathcal{H}_y\{\mathcal{H}_x\{f\}\}D_m^{1,2,3}\right)+\\
&+j\left(\mathcal{H}_x D_m^{1,2,3} + \mathcal{H}_y D_m^{1,2,3}\right)
\end{aligned}
\tag{5}
$$

containing three subbands with positive angle orientations $\text{atan}(1/2)$, $\pi/4$ and $\text{atan}(2)$ and:

$$
\begin{aligned}
&z_{-} = z_{-r} + jz_{-i} =\\
&=\left(f\,D_m^{1,2,3} + \mathcal{H}_y\{\mathcal{H}_x\{f\}\}D_m^{1,2,3}\right)+\\
&+j\left(\mathcal{H}_x D_m^{1,2,3} - \mathcal{H}_y D_m^{1,2,3}\right)
\end{aligned}
\tag{6}
$$

containing three subbands with negative angle orientations $-\text{atan}(1/2)$, $-\pi/4$ and $-\text{atan}(2)$. It can be observed that z_{+} represents the first factor of the first term of the canonical form representation in (1) and that z_{-} represents the first factor of its second term. The main advantage of the proposed implementation of HWT is that this complex transform is reduced at the 2D DWT allowing the heritage of some classes of mother wavelets, like Daubechies, Symmlet or Coiflet families. The quasi shift invariance and the good directional selectivity of the proposed HWT variant are proved in [3].

III. MAP FILTER

The MAP estimation of w, based on the observation $y=w+n$, (where n represents the WT of the noise and w the WT of the useful component of the input image) is given by the MAP filter equation:

$$
\hat{w}(y) = \underset{w}{\text{argmax}}\{\ln(p_n(y-w)p_w(w))\}, \tag{7}
$$

where p_a represents the probability density function (pdf) of a. In the case of the bishrink filter [5] the noise is assumed i.i.d. Gaussian,

$$
p_{\mathbf{n}}(\mathbf{n}) = \frac{1}{2\pi\sigma_n^2}\cdot e^{-\frac{n_1^2+n_2^2}{2\sigma_n^2}}. \tag{8}
$$

The model of the noise-free image in [5] is:

$$
p_{\mathbf{w}}(\mathbf{w}) = \frac{3}{2\pi\sigma^2}\cdot e^{-\frac{\sqrt{3}}{\sigma}\sqrt{w_1^2+w_2^2}}, \tag{9}
$$

a heavy tailed distribution. Each of the vectors **w** and **n** contain two components representing the wavelet coefficients of the noiseless image f and of the noise n localized at the same geometrical positions at the current decomposition level (indexed with 1 and named child coefficients) and at the next decomposition level (indexed with 2 and named parent coefficients). Substituting these two pdfs in the equation of the MAP filter (7) and solving it, the input-output relation of the bishrink filter is obtained as:

$$
{}^{1}\hat{w}_1 = \frac{\left(\sqrt{y_1^2+y_2^2} - \frac{\sqrt{3}\sigma_n^2}{\sigma}\right)_{+}}{\sqrt{y_1^2+y_2^2}}\,y_1. \tag{10}
$$

This estimator requires prior knowledge of the noise variance and of the marginal variance of the clean image for each wavelet coefficient. To estimate the noise variance from the noisy wavelet coefficients, a robust median estimator from the finest scale wavelet coefficients is used [1]:

$$\hat{\sigma}_n = \frac{\text{median}\left(|y_i|\right)}{0.6745}, \quad y_i \in \text{subband HH}. \tag{11}$$

In [5], the marginal variance of the k^{th} coefficient is estimated using neighboring coefficients in the region $N(k)$, a squared shaped window centered on this coefficient with size 7×7. To make this estimation one gets $\sigma_y^2 = \sigma^2 + \sigma_n^2$ where σ_y^2 represents the marginal variances of noisy observations y_1 and y_2. For the estimation of the marginal variance of noisy observations, in [5] is proposed the following relation:

$$\hat{\sigma}_y^2 = \frac{1}{M} \sum_{y_i \in N(k)} y_i^2, \tag{12}$$

where M is the size of the neighborhood $N(k)$. Then σ can be estimated as:

$$\hat{\sigma} = \sqrt{\left(\hat{\sigma}_y^2 - \hat{\sigma}_n^2\right)_+}. \tag{13}$$

A very important parameter of the bishrink filter is the local estimation of the marginal variance of the noise-free image $\hat{\sigma}$. The sensitivity of the estimation $\hat{w}_1$ with $\hat{\sigma}$ is given by:

$$S_{\hat{w}_1}^{\hat{\sigma}_n} = \frac{d\hat{w}_1}{d\hat{\sigma}_n} \cdot \frac{\hat{\sigma}_n}{\hat{w}_1} \text{ or:}$$

$$S_{\hat{w}_1}^{\hat{\sigma}} = \begin{cases} \dfrac{\sqrt{3}\hat{\sigma}_n^2}{\hat{\sigma}\sqrt{y_1^2 + y_2^2} - \sqrt{3}\hat{\sigma}_n^2}, & \text{if } \sqrt{y_1^2 + y_2^2} > \dfrac{\sqrt{3}\hat{\sigma}_n^2}{\hat{\sigma}} \\ 0, & \text{otherwise} \end{cases}. \tag{14}$$

This is a decreasing function of $\hat{\sigma}$. The precision of the estimation based on the use of the bishrink filter decreases with the decreasing of $\hat{\sigma}$.

IV. SIMULATION RESULTS

We compared the performance of the proposed denoising method in terms of output PSNRs for two very well known images: Lena and Barbara, both having the same size 512 × 512 pixels. We have tested four wavelets families: the family of orthogonal wavelets with compact support having the higher number of vanishing moments for the considered support length, denoted in the following by Dau, the family of Symmlets, denoted by Sym, the family of Coiflets denoted by Coif and the family of biorthogonal wavelets denoted by Biort [12]. In our search the Dau family contains 44 elements, the first one being denoted by Dau_4. The family Sym contains 17 elements, the first one being denoted by Sym_4. The family Coif contains 5 members, the first one being denoted by Coif_1. We have also tested 17 pair of biorthogonal wavelets. In each case we have used AWGN with different standard deviations (10, 15, 20, 25, 30 and 35) obtaining different values for the input PSNR (PSNRi) and we have estimated the output PSNRs. In the third step of the denoising algorithm we have computed the Inverse HWT (IHWT) using the algorithm proposed in [13]. The results are presented in Table I. On the first column are given the values of PSNRi. On the second column are presented the output PSNRs obtained with the best mother wavelets from the Dau family. These functions are indexed by the length of the corresponding quadrature mirror filter. On the third column are given the PSNRs obtained using the best mother wavelets from the Biort family. On the fourth column are presented the PSNRs obtained using the best Coiflet. These functions are indexed by their ordering number in the family. Finally, on the last column are highlighted the output PSNRs obtained using the best mother wavelets from the Symm family. They are also indexed by their ordering number in the family. The best results are obtained with the famous biorthogonal pair of mother wavelets Daubechies 9/7. This is one of the pair recommended by the JPEG-2000 image compression standard as well. For the other families, different best mother wavelets are obtained for the treatment of the two different images considered here. The corresponding PSNRs are slightly smaller in comparison with the values obtained using the mother wavelets Daubechies 9/7. To compare the proposed variant of HWT with the 2D DWT, we applied the same denoising procedure based on both WTs in similar conditions (input image, mother wavelets) obtaining the results in following figure. Fig. 2 represents a zoom on a leg with a regular texture from Barbara image. This illustrates that, compared with 2D DWT, the HWT leads to better visual results. Fig. 2(a) corresponding to the 2D DWT is strongly blurred. It clearly appears that the texture with an apparent angle of -π/4 is heavily corrupted by patterns in the opposite direction, due to the mixing in the "diagonal" subband produced in the 2D DWT case.

TABLE I. SIMULATION RESULTS

Lena

PSNRi	Dau_6	Biort9/7	Coif_2	Sym_4
28.17	*35,04*	**35.08**	34.97	35.01
24.66	*33,27*	**33.3**	33.22	33.24
22.13	32,00	**32.04**	31.95	*32.02*
20.23	*31,01*	**31.03**	30.91	30.95
18.61	*30,22*	**30.23**	30.12	30.21
17.30	*29,5*	**29.58**	29.38	*29.5*

Barbara

PSNRi	Dau_14	Biort9/7	Coif_3	Sym_6
28.17	*33.2*	**33.32**	33.17	33.19
24.66	30.93	**31.06**	30.92	*30.94*
22.13	29.32	**29.51**	29.32	*29.33*
20.23	*28.09*	**28.28**	28.09	28.08
18.61	27.09	**27.36**	27.09	*27.10*
17.30	*26.28*	**26.44**	26.24	26.25

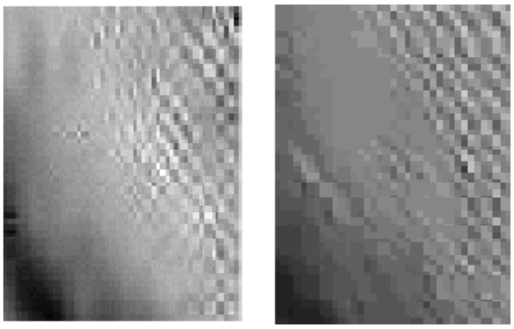

a). b).

Fig. 2. A comparison of the directional selectivity of 2D DWT a) and HWT b).

Details are better preserved in the HWT case, [Fig. 2(b)]. There is much less directional mixture in the HWT case.

V. CONCLUSION

The simulation results reported in this paper are better than the results presented in [3] proving that the bishrink filter is one of the best MAP filters. The proposed variant of HWT outperforms the 2D DWT in denoising applications, due to its quasi shift-invariance and better directional selectivity. The results reported in this paper are inferior with 0.3 dB in comparison with the results reported in [5], where the 2D DTCWT [11] was associated with the bishrink filter. But the architecture in Fig. 1 is simpler than the architecture of the 2D DTCWT, and our algorithm is faster.

The superiority of 2D DTCWT versus the HWT in denoising applications, already mentioned, disappears when the noise is multiplicative as in the case of despecklisation systems. Recent simulations, reported in the PhD Thesis of the first author, prove that the 2D DTCWT and the HWT can be considered equivalent in despecklisation applications.

The blurring effect introduced by the HWT can be reduced by substituting the 2D DWTs in Fig. 1, by other 2D WTs with better frequency localization like for example the 2D Wavelet Packets Transform (2D WPT) [14]. This flexibility is another very fine feature of the HWT. The four 2D DWTs in figure 1 can be substituted directly by other WTs, like the 2D WPT or the 2D M-band WT. The HWT can be regarded as a Gabor's filter bank [15].

We have searched here the best mother wavelets following a classical approach based on trials. We have found results compatible with the whole noiseless image. This strategy could be applied for other image processing methods as well. For example we have applied it for the images watermarking in [16].

The searching strategy can be enhanced considering the variability of natural images. They are composed by different structures: homogeneous regions, textured regions and contours. Each type of structure has a set of features and can be associated with best mother wavelets. So, a refined strategy for the search of the best mother wavelets segments first a partial denoising result (obtained using the mother wavelets Daubechies 9/7 for example) to identify the structures composing the noiseless component of the image under processing. Next the features of each structure are identified and the corresponding mother wavelets are searched. Finally each corresponding structure of the noisy image is denoised using its corresponding best mother wavelets. The identification of the structures and of their features can be done using the algorithm proposed in [17]. The searching of the best mother wavelets for textured regions can be done following the method proposed in [18]. The searching of the best mother wavelets for homogeneous regions and for contours can be done on the basis of their time-frequency localization. The best mother wavelets for the processing of such a structure could be mother wavelets with the same time-frequency localization. In [19] are estimated the time-frequency localizations of the elements of the Daubechies family denoted in the present paper by Dau. Based on this classification in [20] is proposed an enhancement of the proposed denoising method by diversification followed by fusion.

ACKNOWLEDGMENT

The research reported in this paper was developed in the framework of a grant funded by the Romanian research council (CNCSIS) with the title "Using wavelets theory for decision making" no. 349/13.01.09.

REFERENCES

[1] D. L. Donoho and I. M. Johnstone, "Ideal spatial adaptation by wavelet shrinkage", Biometrika, 81(3), pp. 425-455, 1994.

[2] Foi, A., V. Katkovnik and K. Egiazarian, "Pointwise Shape-Adaptive DCT for High-Quality Denoising and Deblocking of Grayscale and Color Images", IEEE Trans. Ima. Proc., (5), 1395-1411, 2007.

[3] Firoiu I., Nafornita C., Boucher J. –M., Isar A., "Image Denoising Using a New Implementation of the Hyperanalytic Wavelet Transform," IEEE Transactions on Instrumentation and Measurements, vol. 58, Issue 8, pp. 2410-2416, August 2009.

[4] S. Foucher, G. B. Benie and J.-M. Boucher, "Multiscale MAP Filtering of SAR images", IEEE Trans. Ima. Proc., vol. 10, no.1, pp. 49-60, 2001.

[5] L. Sendur and I. W. Selesnick, "Bivariate shrinkage functions for wavelet-based denoising exploiting interscale dependency", IEEE Trans. on Signal Processing, 50(11), pp. 2744-2756, 2002.

[6] F. Luisier, T. Blu and M. Unser, "A New SURE Approach to Image Denoising: Inter-Scale Orthonormal Wavelet Thresholding", IEEE Trans. Ima. Proc., vol.16, no. 3, pp. 593-606, 2007.

[7] A. M. Atto, D. Pastor and G. Mercier, Smooth Sigmoid Wavelet Shrinkage For Non-Parametric Estimation, *IEEE International Conference on Acoustics, Speech and Signal Processing, ICASSP,* Las Vegas, Nevada, USA, 30 march - 2008.

[8] Ebrahimzadeh, A., Khazaee, A., An Efficient Technique for Classification of Electrocardiogram Signals, Advances in Electrical and Computer Engineering Journal, no. 3, pp. 89-93, 2009.

[9] S. C. Olhede and G. Metikas, „The hyperanalytic wavelet transform," Dept. Math., Imperial College, London, U.K. Imperial College Statistics Section Tech. Rep. TR-06-02, May 2006.

[10] C. Davenport, Commutative Hypercomplex Mathematics, http://home.comcast.net/~cmdaven/hyprcplx.htm .

[11] N. Kingsbury, Complex Wavelets for Shift Invariant Analysis and Filtering of Signals, Applied and Comp. Harm. Anal. 10, pp. 234-253, 2001.

[12] I. Daubechies, Ten Lectures on Wavelets, SIAM, Philadelphia, 1992.

[13] Ioana Firoiu, Alexandru Isar, Jean-Marc Boucher, An Improved Version of the Inverse Hyperanalytic Wavelet Transform, Proceedings of IEEE International Symposium SCS'09, Iasi, Romania, July 9-10, pp. 13-16, 2009.

[14] Firoiu I., Isar D., Boucher J.-M., Isar A., "Hyperanalytic Wavelet Packets," Proc. IEEE Conf. WISP 2009, Budapest, Hungary, pp. 67-72, 2009.

[15] Lajevardi, S.M., Hussain, Z. M., Feature Extraction for Facial Expression Recognition based on Hybrid Face Regions, Advances in Electrical and Computer Engineering Journal, no. 3, pp. 63 – 67, 2009.

[16] Nafornita C, Isar A., "On the Choice of the Mother Wavelet for Perceptual Data Hiding," Proceedings of IEEE International Symposium SCS'09, Iasi, Romania, July 9-10, pp. 233-236, 2009.

[17] Wan T., Canagarajah N., Achim A., „Segmentation-Driven Image Fusion Based on Alpha-Stable Modeling of Wavelet Coefficients," IEEE Transactions on Multimedia, vol. 11, no. 4, pp. 624-633, June 2009.

[18] G.C.K. Abhayaratne, I. H. Jermyn and J. Zerubia, "Texture-adaptive mother wavelet selection for texture analysis", *Proc. IEEE International Conference on Image Processing (ICIP)*, Genova, Italy, September 2005.

[19] Oltean M., Isar A., "On the Time-Frequency Localization of the Wavelet Signals with Application to Orthogonal Modulation," Proceedings of IEEE International Symposium SCS'09, Iasi, Romania, pp. 173-176, July 9-10, 2009.

[20] Firoiu I., Isar A., Isar D., "A Maximum A Posteriori Approach of Hyperanalytic Wavelet Based Image Denoising in a Multi-Wavelet Context," Proceedings of the 9th WSEAS International Conference on Signal Processing (SIP '10), Catania, Italy, May 29-31, 2010.